Species boundaries of the predaceous chub *Parazacco spilurus* (Xenocyprididae) and the description of a new cryptic species from southern China

Jeffery C.F. Chan*[1,2], Bi Wei Low[2,3], Jia Huan Liew*[2,4], Heok Hui Tan[5]

[1]School of Biological Sciences, The University of Hong Kong, Hong Kong; ([*]corresponding author: J.C.F. Chan, email: jefferychan@connect.hku.hk; ORCID 0000-0003-0412-9429).
[2]Science Unit, Lingnan University, Hong Kong.
[3]Department of Biological Sciences, Faculty of Science, National University of Singapore, Singapore; (email: biweilow@gmail.com; ORCID 0000-0002-2549-4938).
[4]School of Natural Sciences, University of Tasmania, Private Bag 51, Hobart, Tasmania, 7001, Australia; ([*]corresponding author, J.H. Liew, email: JiaHuan.Liew@utas.edu.au; ORCID 0000-0002-7649-0398).
[5]Lee Kong Chian Natural History Museum, National University of Singapore, Singapore, Singapore; (email: heokhui@nus.edu.sg; ORCID 0000-0003-2227-8866).

Abstract

The East Asian minnow genus *Parazacco* are ecologically and economically valuable riverine fishes, distributed from southern China to northern Vietnam. The type species, *P. spilurus* has suffered from overexploitation and habitat loss, with evidence of being in a species complex. Using genome-wide SNPs and morphological characters, several populations of *P. spilurus* from Hong Kong, Southern China were examined and the existence of an undescribed cryptic species (described herein as ***Parazacco ignis* sp. nov.**) was verified. Low levels of hybridisation between the two species were found and their presence was not prevalent within contact zones. The status of the type material of *P. spilurus* was also examined and a neotype is proposed along with a redescription using mature specimens to stabilise the taxonomy, owing to the poor condition and juvenile life stage of the syntypes. ***Parazacco ignis* sp. nov.** differs from *P. spilurus* in adult life coloration, genetics, and several morphological characters. The misidentification of *P. spilurus* has important conservation implications, given the overestimation of its current distribution and historic population declines. Comprehensive integrative taxonomy across the entire range of the genus is recommended to reassess species distributions and clarify taxonomic status.

Keywords: Species complex; integrative taxonomy; freshwater fish; southern China; ddRADseq; morphology

Introduction

Parazacco is an ecologically and economically valuable genus of freshwater minnow-like fishes, ranging from southern China to northern Vietnam (Wang et al. 1998; Kottelat, 2001). It is a widely distributed top predator that plays a significant role in shaping species assemblages and is an indicator of intact riparian forests in the streams of Hong Kong, southern China (Chan et al., 2005; Lau et al., 2009; Chan et al., 2024). The type species, *Parazacco spilurus* has suffered from historic population decline across China over the last century, owing to overexploitation and habitat degradation, but has been revised from 'Vulnerable' to 'Least Concern' in the China Species Red List since 2016 (Wang et al., 1998; Jiang et al., 2016).

The genus *Parazacco* (Chen, 1982) belongs to the opsariichthine group of East Asian minnows; comprising only two known species: *Parazacco spilurus* Günther, 1868 and *Parazacco fasciatus* Koller, 1927 (Kottelat, 2013; Wang et al., 2019). *Parazacco spilurus* was described from "inland mountainous regions of Hong Kong" by Günther (1868) based on five juvenile syntypes (29.0 – 44.5 mm SL; Ito and Hosoya, 2016). *Parazacco fasciatus* was initially described as a subspecies based on 14 specimens from Kang-Kong River, Hainan Island, southern China (~500 km from Hong Kong) by Koller (1927). It was subsequently elevated to species status in Kottelat (2001) and maintained in Kottellat (2013). However, *P. fasciatus* was treated as a synonym of *P. spilurus* by Ito and Hosoya (2016) despite differences in diagnostic features because of concerns of allometric growth when comparing the juvenile *P. spilurus* syntypes with the large (90 – 140mm TL; Koller, 1927) mature holotypes and paratypes of *P. fasciatus* in Koller (1927). Nonetheless, Wang et al. (2019) agreed with Kottelat (2001) and Kotelat (2013) that the two species were valid based on evidence from mitochondrial cytochrome b (cyt b) sequences.

However, recent molecular analyses of the mitochondrial control region, cyt b, and nuclear recombination-activating gene 1 of *P. spilurus* from Hong Kong suggest that there are two highly divergent lineages with low levels of hybridisation (Wu et al., 2019). The inclusion of *P. fasciatus* sequences with the two *P. spilurus* lineages from Hong Kong yielded significant divergences (> 3%) among the three groups, indicating the presence of at least three, rather than two distinct species in the genus (Wu, 2017).

The presence of a cryptic species has major implications on the management of *P. spilurus*, as its population range has likely been overestimated. Despite this, work on the undescribed cryptic species in Hong Kong is limited by the poor condition of the *P. spilurus* syntypes (bleached, damaged scales and fins), and more significantly, by the fact that the syntypes are juveniles that lack diagnostic features (e.g., immature specimens will not have tubercules or certain coloration) and undergo allometric growth that may lead to morphological variations (Osse and Van den Boogaart, 1995). This issue is compounded by the vague description of the locality of the syntypes by Günther (1868) being in "inland mountainous regions of Hong Kong" as *Parazacco* spp. are widespread in the region (AFCD, 2025).

To resolve the current state of *Parazacco spilurus*, a comprehensive integrative taxonomy approach was undertaken to: (i) verify the presence of two distinct species in Hong Kong using double digest restriction-site associated DNA sequencing (ddRADseq) and traditional morphomeristics; (ii) identify the degree of hybridization between *P. spilurus* and the undescribed species; (iii) stabilize the taxonomy of *Parazacco*, by designating a neotype with an adult *P. spilurus* from central New Territories and the redescription of *P. spilurus* from mature specimens; (iv) describe the new cryptic species.

Methods

Fishes were collected from 13 sites around Hong Kong with reference to Wu et al., (2019) (Table 1; Fig. 1) with permits from the Agriculture, Fisheries, and Conservation Department of the HKSAR Government (AF GR CON 11/17 Pt. 7). Specimens were euthanised in the field using MS 222, following Underwood and Anthony (2020). Caudal fin clips were extracted from 5–13 specimens per population for DNA extraction (Table 1). Specimens for morphomeristic analyses

were brought back to the laboratory and fixed in 10% formalin for two weeks, rinsed in tap water, then stored in 70% ethanol.

DNA was extracted using the Qiagen Blood & Tissue Kit following the manufacturer's protocol and quantified using Qubit 2.0 Broad Range DNA Assay. RADseq library preparation followed a modified protocol of Peterson et al. (2012) (EcoRI and MspI as restriction enzymes; Tight 350bp size selection settings using Pippin-Prep). Specimens were then sent to NovogeneAIT Genomics Shanghai for sequencing using the NovaSeq X Plus. Lanes were spiked with 40% PhiX to increase nucleotide diversity.

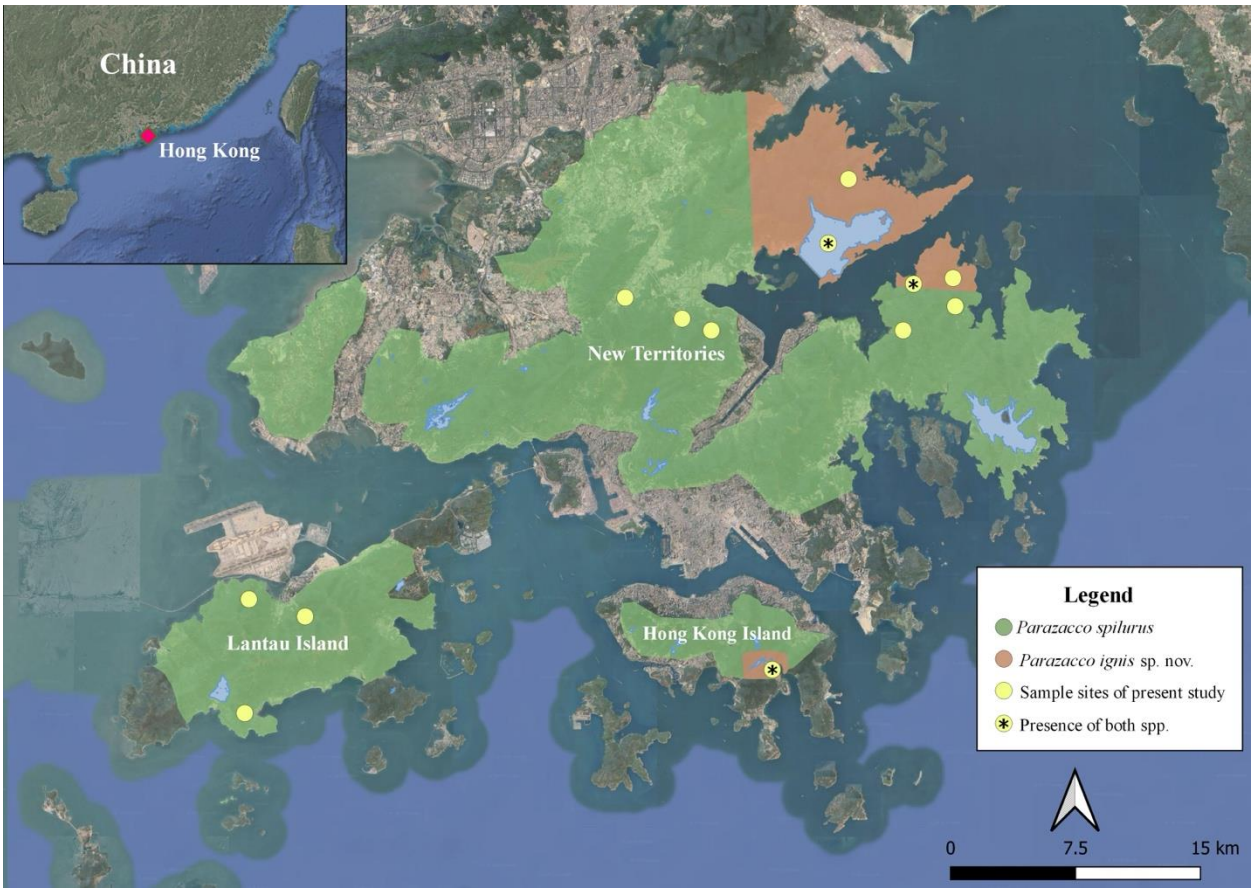

Figure 1. Sample sites of *Parazacco spilurus* and *P. ignis* sp. nov. in Hong Kong from the present study. Green and red shading represent approximate distributions of both species in Hong Kong inferred from Wu et al. (2019) and AFCD (2025).

SNP identification

Raw paired-end reads were demultiplexed using the 'process_radtags' module in Stacks version 2.61 (Rochette et al., 2019) and assembled against the chromosome-level assembly of *Opsariicthys bidens* (Liu et al., 2022) using the 'bwa-mem' algorithm in Burrows-Wheeler aligner version 0.7.17 (Li and Durban, 2009). Aligned sequences were sorted to coordinate order using samtools version 1.17 (Li et al., 2009), and single nucleotide polymorphisms (SNPs) were then called using the 'ref_map.pl' pipeline and 'populations' module in Stacks. Only the first SNP per locus and loci that were present in ≥ 50% samples were retained (Paris et al., 2017). Further filter criteria

were applied in PLINK version 1.90 (Purcell et al., 2007) to remove SNPs with >50% loci missing, in Hardy-Weinberg Equilibrium (HWE; $P < 0.05$), and those that are unlinked.

Population genomic analyses

Patterns of genetic clustering among samples were first examined using PCAs in the R environment version 4.41 (R Core Team, 2024) with the 'SNPRelate' (Zheng et al., 2012) package. A Bayesian clustering approach in Structure version 2.3.4 (Pritchard et al., 2000), was then used to infer population structure within the dataset. The admixture-locprior model was used, with 100,000 burn-in and 200,000 Markov chain Monte Carlo (MCMC) iterations, testing for K (number of genetic clusters) values of 1–6 with ten replicates per K value. Structure runs were averaged and summarized using CLUMPAK (Kopelman et al., 2015), and the uppermost level of population structure was identified using the Evanno Δ method (Evanno et al., 2005). A co-ancestry similarity matrix was then calculated by utilizing haplotype linkage information and focusing on the most recent coalescence (common ancestry) among individuals using the fineRADstructure pipeline (Malinsky et al., 2018). The 'populations' program in STACKS was used to filter haplotypes (locus present in ≥ 75% samples) before input into the fineSTRUCTURE MCMC clustering algorithm with 100,000 burn-ins and sample iterations, respectively.

Hybrid detection

The R package 'hybriddetective' (Wringe et al., 2017a) was used to identify hybrids and hybrid classes (pure, F1, F2 or backcrosses) where interspecific gene flow was detected. Separate panels of 100, 200, and 300 SNPs with the highest interspecific fixation index (F_{ST}) and not in linkage disequilibrium were extracted from a subsetted dataset of pure individuals (inferred from Structure admixture plots) from both species. Three independent simulations of multigenerational hybrids (pure individuals, F1, F2, and backcrosses of hybrids with pure individuals) were then replicated three times each followed by 50,000 burn-ins and 200,000 MCMC sweeps using the R package 'parallelnewhybrid' (Wringe et al., 2017b). Each panel's accuracy (individuals correctly assigned to a class/ total number of individuals assigned to a class) and efficiency (no. hybrids detected / no. hybrids in sample) (Vähä and Primmer 2006) were evaluated in 'hybriddetective' using the 'hybridPowerComp' function (Wringe et al., 2017a) to select the optimal panel size. Simulated subsetted individuals of the selected panel size were then combined with the full dataset to assign all individuals into hybrid classes with 50,000 burn-in and 100,000 MCMC sweeps using 'parallelnewhybrid'.

Phylogenomic analyses

Species-level maximum likelihood phylogenies were inferred in SNAPP version 1.4.0 (Bryant et al., 2012), as implemented in BEAST (Drummond and Rambaut, 2007) with 500,000 MCMC iterations. Phylogenies were based on a subset of individuals from each species with *Acrossocheilus beijiangensis*, *A. parallens*, *Opsariichthys evolans*, and *O. bidens* as outgroups (Table 1). External time calibrations between *Parazacco* and *Opsariichthys* of (~22.6 mya were used in this analysis (Cheng et al., 2022). A maximum clade credibility (MCC) tree was then generated with the program 'TreeAnnotator' version 1.10 (Helfrich et al., 2018), using a burn-in of the first 10% of each MCMC chain, and visualized with the program 'FigTree' v.1.4.3 (Rambaut, 2016).

Morphomeristics

Methods for counts and measurements follow Hubbs and Lagler (2004) as modified by Armbruster (2016). Measurements were made point-to-point using dial calipers, and recorded to the closest 0.1 mm. All counts and measures were taken on the left side of the body. Abbreviations are as follows: TL = total length, SL = standard length, HL = head length. Radiographs were obtained using a Faxitron LX-60 cabinet X-ray system. Vertebral counts follow Roberts (1989) with a count of three added for the Weberian complex. See Table 1 for specimens examined.

Results

For our population genomic analyses, A total of 88 *Parazacco* individuals were sequenced for population genomic analyses, with an average sequencing coverage of 93x per sample (range of 10–142x). After our filtering step (retaining only unlinked SNPs in HWE, and individuals with <50% missing data), a total of 6,877 SNPs and all 88 individuals were retained for downstream analyses. For our phylogenetic analyses, we sequenced six *P. spilurus*, three *Parazacco ignis* sp. nov., two *Opsariichthys evolans*, one *O. bidens*, three *Acrossocheilus beijiangensis* and one *A. parallens*, with an average sequencing coverage of 98x per sample (range of 35–141x). After filtering, we retained 1,005 SNPs and all 15 individuals.

Population genomic analyses

Clustering analyses using STRUCTURE identified the best number of genetic clusters at K = 3 based on the Evanno ΔK method (ΔK of 4619.9 for K=2, 398461.8 for K=3 and 0.3 for K=4; Fig. 2A). At K = 2, *P. spilurus* (blue, Fig. 2A) and *Parazacco ignis* sp. nov. (orange) were distinctly separated. At K = 3, additional population structure was detected in *P. spilurus* from Lantau Island, whilst *P. ignis* sp. nov. remained the same. At K = 4, further structuring was detected in *P. spilurus* from the eastern and north-eastern New Territories. The PCA (Fig. 2B) showed four main clusters with the first principal component (PC1, 35.1% variance explained) delimitating *P. spilurus* from *P. ignis* sp. nov. and PC2 (9.3% variance explained) separating *P. spilurus* into three groups.

Recent co-ancestry at the individual haplotype level from the results of fineRADStructure (Fig. 3A) showed that *Parazacco* populations formed two distinct clusters with low levels of haplotype sharing, with individuals from SH, WLH, LT, TP, TPK, CT, and YSO in one cluster (*P. spilurus*) and CT, HH, SAC in another (*P. ignis* sp. nov.), which are in parallel with the K = 2 STRUCTURE plot (Fig. 1A). Two contact zones were also identified (LCC and PC; Fig. 2–3) including two putative hybrids from LCC (LCC1 and LCC5). The mean observed and expected heterozygosity was higher in sites with only *P. spilurus* (H_o = 0.042, H_e = 0.045) than only *P. ignis* sp. nov. (H_o = 0.023, H_e = 0.017) (Table S1). The highest mean observed and expected heterozygosity were recorded in the two contact zones (H_o = 0.094, H_e = 0.306; Table S1).

Hybrid detection

The 200 SNP panel was selected for hybrid identification due to having the highest accuracy and efficiency (Figs S1–S2). A total of two hybrids were detected from 1 of 13 sites (LCC; Fig. 3B) and coincide with the two individuals inferred from the STRUCTURE plot, PCA biplot, and co-ancestry matrix (Figs 2–3). Hybrid classification indicated that both hybrids were most likely backcrosses with *P. spilurus*, of which one individual had a low probability of being an F2 hybrid. No F1 hybrids or backcrosses with *P. ignis* sp. nov. were detected.

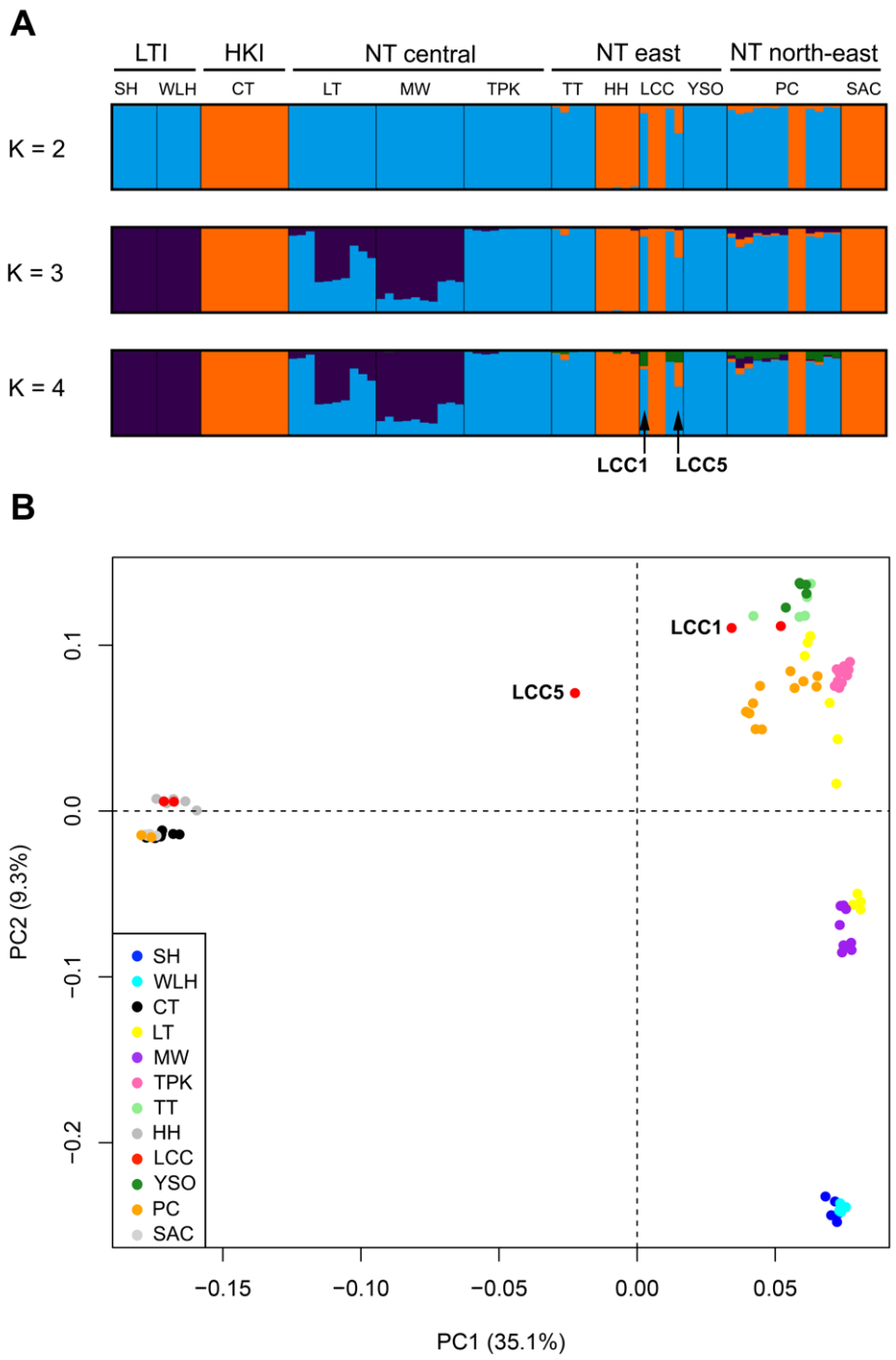

Figure 2. **(A)** Structure plot of *Parazacco* populations in Hong Kong; K = 3 was identified to be the optimal K value based on the Evanno ΔK method; **(B)** Genetic clustering of *Parazacco* individuals from Hong Kong, as inferred from PCA; each point represents an individual sample and each color represents a sampling locality. Two putative hybrids, LCC1 and LCC5, are labelled. Please see Table 1 for site abbreviations.

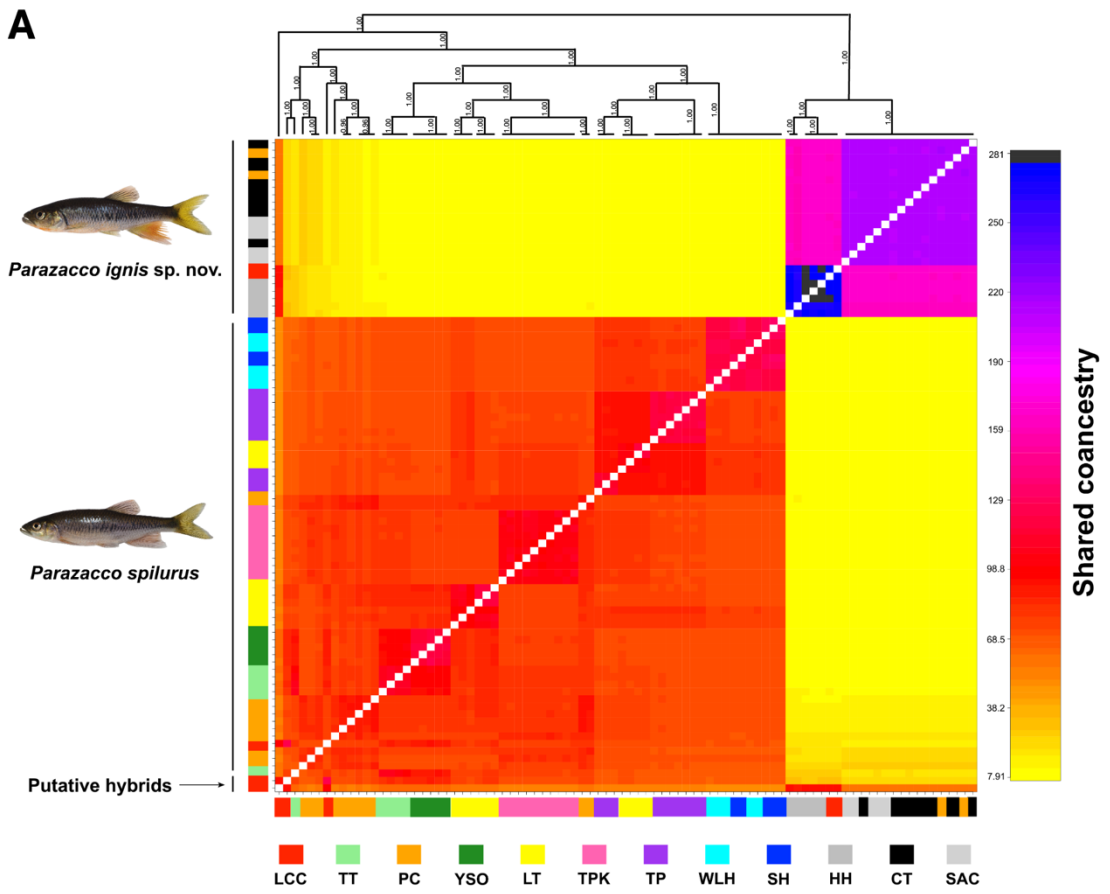

Figure 3. (**A)** FineRADstructure co-ancestry matrix calculated using genome-wide SNPs; each row/column represents a single individual with labels indicating the location of the individual; horizontal and vertical axes are rotations of one another; yellow represents the lowest levels of recent common ancestry between individuals, whereas black represents the highest levels of recent shared ancestry; the Bayesian MCMC tree is displayed at the top, with posterior population assignment probabilities given; (**B)** Hybrid analysis of *Parazacco spilurus*, *P. ignis* sp. nov., and hybrids using 'hybriddetective' and 'parallelnewhybrid'; F1 hybrid: first-generation hybrids (not detected in this study); F2 hybrid: second generation hybrids; Backcross 1: backcross of hybrid to pure *P. spilurus*; BC2: backcross of hybrid to pure *P. ignis* sp. nov. (not detected in this study); see Table 1 for site abbreviations.

Species tree

The maximum clade credibility SNAPP tree was well-supported with extremely high Bayesian posterior probabilities throughout (Fig. 4). The final tree topology showed that our specimens formed three main clades that corresponded to the genera *Parazacco*, *Opsariichthys*, and *Acrossocheilus*, with the former two being sister taxa. Within-clade relationships were unambiguous and divergence time estimates showed that the two *Parazacco* lineages diverged ~4.87 mya, which is comparable to lineage divergence within *Opsariichthys* (~6.03 mya) and *Acrossocheilus* (~4.96 mya).

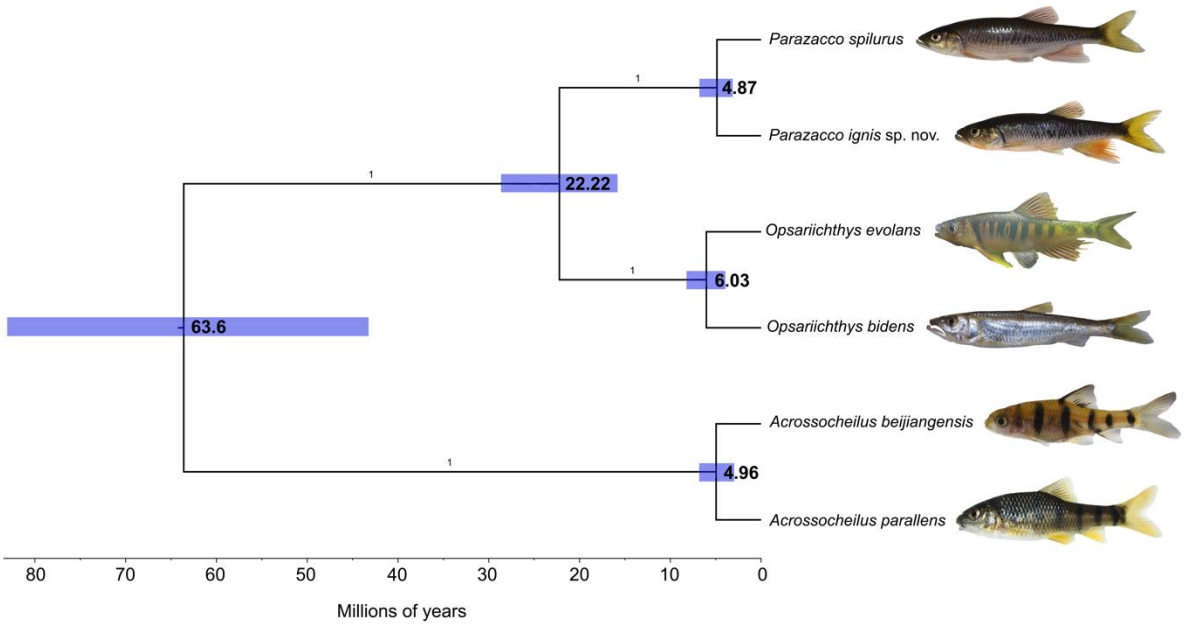

Figure 4. Phylogeny and estimate divergence times of *Parazacco spilurus*, *P. ignis* sp. nov, and four outgroup species (*Opsariicthys evolans*, *O. bidens*, *Acrossocheilus beijiangensis*, and *A. parallens*). Branch labels indicate Bayesian posterior probabilities, whereas node labels and node bars are mean and 95% highest posterior densities of node ages, respectively.

Morphomeristics

A total of 42 specimens underwent morphometric analyses (Table 1). *Parazacco spilurus and P. ignis* sp. nov were differentiated using a suite of four characters. Diagnostic characters included caudal peduncle length % SL, upper jaw length % HL, and lateral line and pre-dorsal scale counts (Fig. 5; Table 2). Further comparisons were made with types of *P. fasciatus* described in Koller (1927) and Ito and Hosoya (2016), which showed that *P. spilurus and P. ignis* sp. nov. exhibited several non-overlapping character differences with *P. fasciatus*: head length % TL; body depth % TL; dorsal fin ray counts; anal fin ray counts; and pelvic fin ray counts (Table 2). Given the poor condition and juvenile life stage of the syntypes *Parazacco spilurus* Günther, 1868, a neotype is proposed (based on recent material collected from the presumed type locality area) and a redescription is provided from adult specimens to provide a reference for future studies and stabilise the taxonomy of the species. Following which, *Parazacco ignis* sp. nov. is described.

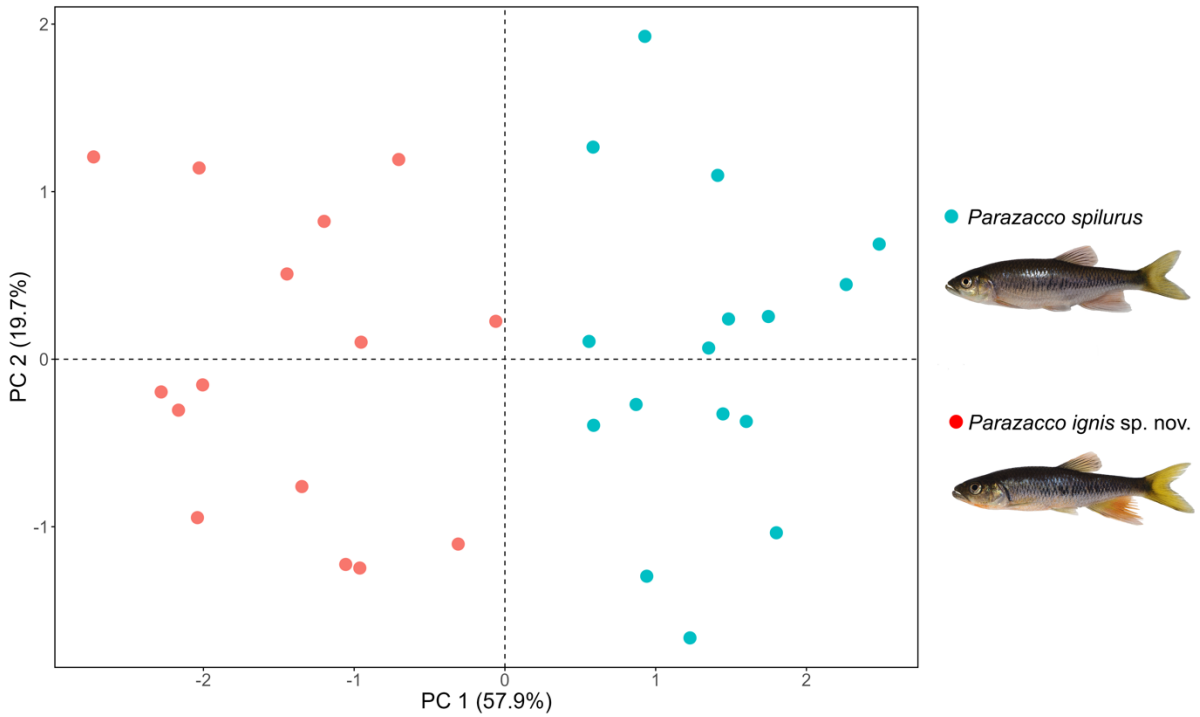

Figure 5. Principal components analysis of *Parazacco spilurus* and *P. ignis* sp. nov. using four distinguishing features (caudal peduncle length % SL, upper jaw length % HL, and lateral line and pre-dorsal scale counts).

Taxonomic account
Order Cypriniformes Goodrich, 1909
Family Xenocyprididae Günther, 1868
Genus Parazacco Chen, 1982

Parazacco spilurus (Günther, 1868)
(Figs. 6–8, Tables 2–3)

Aspius spilurus Günther, 1868

Proposed neotype: ZRC 68029, 99.2 mm SL, Ma Wo, foothills of Tai Mo Shan, central New Territories, Coll. J. C. F. Chan and B. W. Low.

Material examined. BMNH 1956.2.25.1–5 (5 syntypes; X-rays from BMNH Data portal; data and pictures from Ito and Hosoya (2016)); ZRC 68034, 4 ex., 50.9–122.1 mm SL, Yung Shue O, New Territories, Coll. J. C. F. Chan; ZRC 68033, 4 ex., 69.6–81.0 mm SL, San Tau, Lantau Island, Coll. J. C. F. Chan; ZRC 68035, 5 ex., 77.7 – 108.0 mm SL, Shui Hau, Lantau Island, Coll. J. C. F. Chan; ZRC 68032, 7 ex., 16.5 – 82.2 mm SL, Tai Tan, New Territories, Coll. J. C. F. Chan; ZRC 68030, 2 ex., 29.4 – 49.0 mm SL, Ma Wo, New Territories, Coll. J. C. F. Chan and B. W. Low. *Parazacco fasciatus*: X-ray and pictures of holotype and 12 syntypes from A. Palandačić, NMW; data on the same specimens from Koller (1927) and Ito and Hosoya (2016).

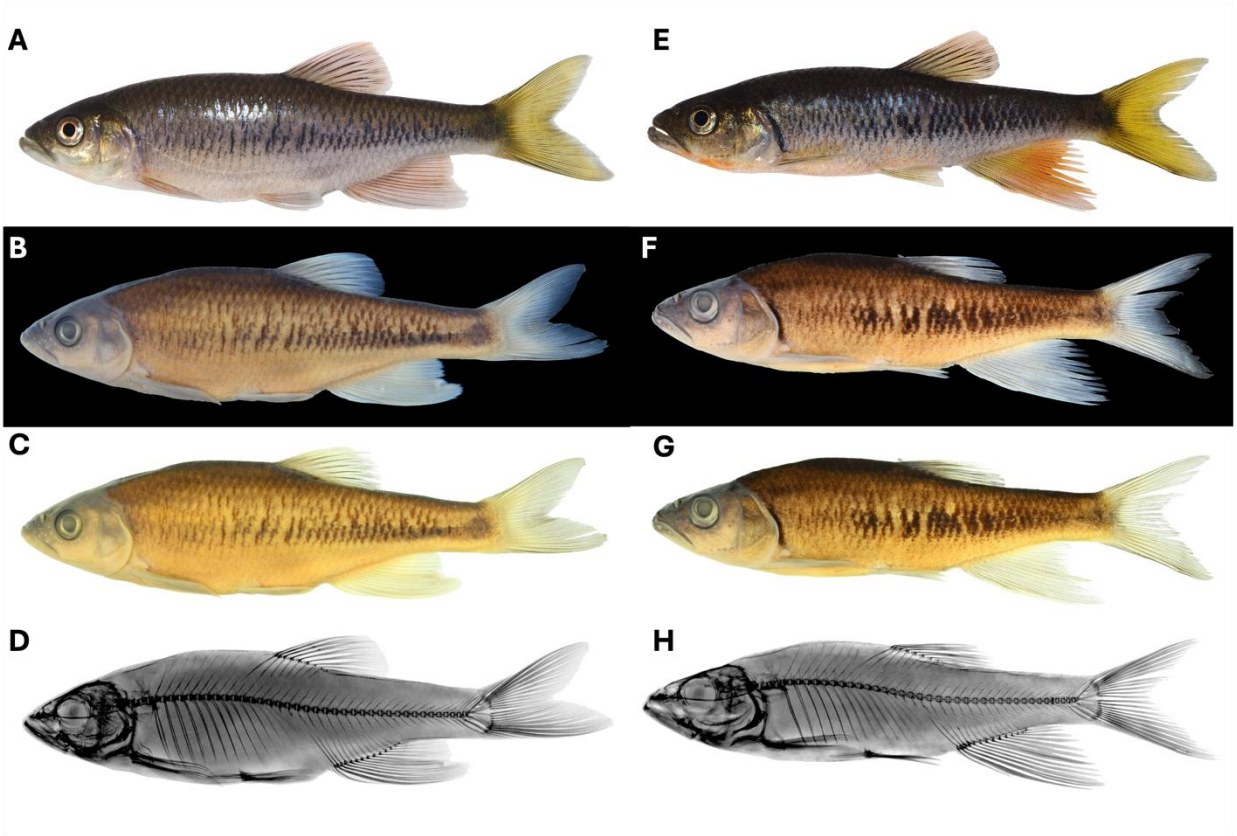

Figure 6. *Parazacco spilurus*, proposed neotype 99.2 mm SL; Hong Kong, New Territories, Ma Wo; **(A)** freshly dead fish; **(B)** preserved fish on black background, **(C)** preserved fish on white background; **(D)** positive radiograph; *Parazacco ignis* sp. nov., holotype 96.5 mm SL; Hong Kong, New Territories, Sam A Chung; **(E)** freshly dead fish, **(F)** preserved fish on black background; **(G)** preserved fish on white background; **(H)** positive radiograph.

Diagnosis. *Parazacco spilurus* can be distinguished from *P. fasciatus* by having a shorter head (20.3 – 26.5 % TL vs 28) that is less compressed and more downward-pointed (Fig. 7), slimmer body (17.3 – 22.6 % TL vs 25), shorter snout (28.7 – 36.0 % HL vs 35.7 – 43.4), more pelvic fin rays (7 – 9 vs 6), and more lateral line scales (45 – 50 vs 41 – 44) (Koller, 1927; Ito and Hosoya, 2016). *Parazacco spilurus* can be distinguished from *P. ignis* sp. nov. by the following combination of features in specimens > 50 mm SL: longer caudal peduncle length (16.0 – 19.5% SL vs 15.1 – 18.8); longer upper jaw length (41.4 – 46.5% HL vs 38.2 – 43.9); more lateral line scales (mode 46 vs mode 43); more pre-dorsal scales (mode 22 vs mode 20) (Fig. 7; Table 2); more tubercules on the lower jaw extending to the lower cheek and are evenly sized (mode 4 vs mode 2 and significantly larger first and last tubercules); top of head is more compressed; black lateral stripe appears to be more solid in juveniles (*vs* more blotchy; Fig. 8); and no coloration to minimal red-orange specks of the chin extending to the belly in specimens < 80 mm SL (vs clear presence of red-orange coloration; see Fig 6).

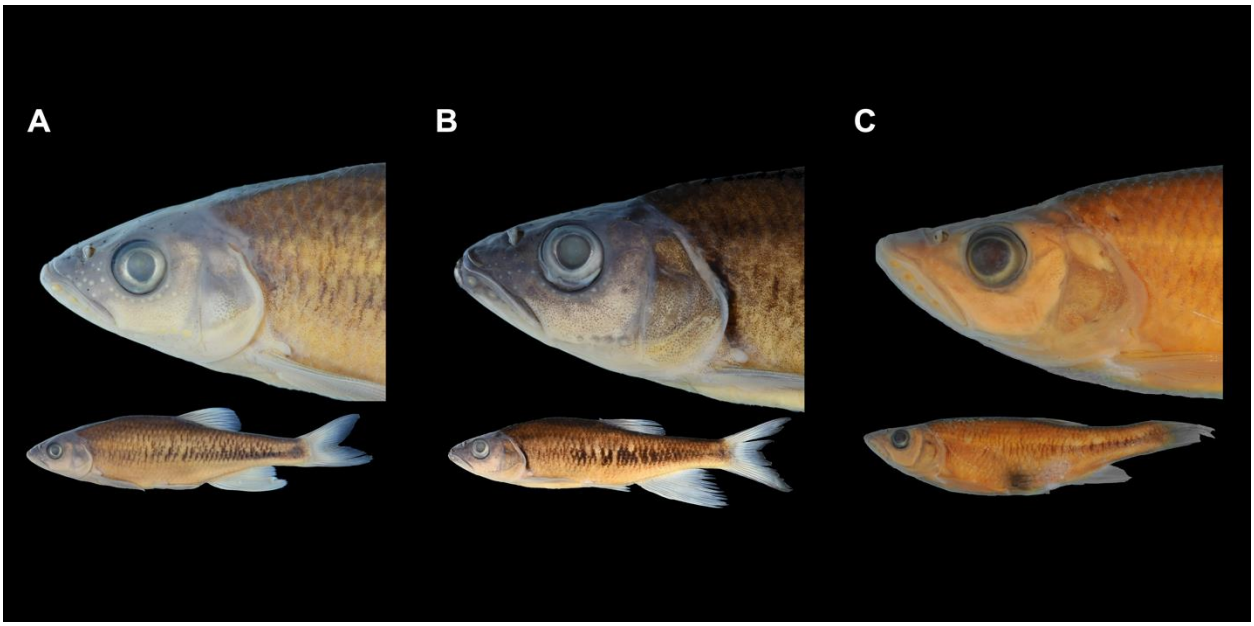

Figure 7. Lateral head close-up and full lateral body of **(A)** *Parazacco spilurus* proposed neotype; **(B)** *P. ignis* sp. nov. holotype; **(C)** *P. fasciatus* paratype NMW10407-419_paratype_3 (photographs provided by A. Palandačić, NMW).

Redescription. Morphometric data is given in Tables 2 – 3. Meristic data are as follows: 7 dorsal fin rays; 11 (3) – 12 (13) anal fin rays; 13 (11) – 14 (5) pectoral fin rays; 7 (9) – 8 (7) pelvic fin rays; 45 (2), 46 (6), 47 (4), 48 (1), 49 (2), or 50 (1) lateral line scales; 9 (11) – 10 (5) scales above lateral line; 3 (12) – 4 (4) scales below lateral line; 21 (2), 22 (6), 23 (5), 24 (3) pre-dorsal scales; 8 (7), 9 (7), or 10 (2) caudal peduncle scales; 3 (1), 4 (4), 5 (2), 7 (1), 8 (1), 9 (2), 10 (2), or 11 (3) tubercles on lower jaw and cheek; vertebral count 19 – 21 + 20–21 = 41 (3), 42 (9), or 43 (8). Measurements of the neotype and material are provided in Table 3.

General body form as in Fig. 6A – D. Body elongate and laterally compressed. Head somewhat depressed. No maxillary barbels. Eyes rather large. Upper lip notched with prominent front edge of lower jaw. Tubercles distinct on head and present in all specimens < 50 mm SL, with a single row of 3 – 11 tubercles on lower jaw that extends just before the opercle; tubercles also present on snout and as a row above the upper lip extending to under the eyes before the opercle. Body with cycloid scales and complete lateral line, which abruptly runs downward just above the pectoral fin and extends into middle of caudal fin base. Supra-pectoral and supra-pelvic flaps present.

When alive, light to dark grey starting from the lower lip, through the snout and dorsal body, gradually turning white on the lateral sides below the lateral line. A black horizontal stripe runs above the lateral line from the gills to the caudal peduncle and is most prominent in juveniles before fading from anterior to posterior among larger the specimen. Black vertical stripe on operculum and black spot on caudal peduncle, which is also most prominent in juveniles before fading with maturation. All fins pale yellow and become increasingly vibrant with increasing size. Red-orange coloration develops in dorsal and anal fins in more mature specimens > ~80 mm SL but does not have prominent coloration under the throat to across the belly.

When preserved, head and dorsal body retains light grey and becomes paler on the lateral side below the lateral line. Black spot on caudal peduncle becomes more apparent. Fins lose red-orange coloration, but dark oblong bands between dorsal fin rays remain.

Habitat. Lowland and inland mountainous streams up to ~500m in elevation.

Distribution. Known with certainty to be widely distributed in Hong Kong (Lantau Island, New Territories, Hong Kong Island; Fig. 1). Possibly distributed in the Longjin, Beijiang, and Dongjiang systems in Guangdong Province, China (Pan et al., 1991). Also reportedly found in southern Fujian to southern Guangxi province (Li et al., 2003).

Parazacco ignis sp. nov.
(Figs 6 – 8; Tables 2 and 4)

Parazacco spilurus (non-Günther) **–** Günther, 1868; Man and Hodgkiss, 1981 (part); Chong and Dudgeon, 1992 (part); Lee et al., 2004 (part); Tsang and Dudgeon, 2021 (part).

Zoobank registration: urn:lsid:zoobank.org:pub:69C34647-AFDD-4D45-8440-F63CDD93F24F

Holotype. ZRC 68036, 96.5 mm SL, Sam A Chung stream, New Territories, Coll. J. C. F. Chan et al., 19 Jan. 2022.

Paratypes. ZRC 68037, 40 ex., 14.0 – 74.7 mm SL, Sam A Chung, New Territories, Coll. J. C. F. Chan et al., 19 Jan. 2022; ZRC 68039, 17 ex., 14.6 – 80.6 mm SL, Hoi Ha, New Territories, Coll. J. C. F. Chan; ZRC 68038, 5 ex., 82.1 – 92.7 mm SL, catchwater-fed stream (Chai Tai) ~500m from Tai Tak Tuk Reservoir, Tai Tam, Hong Kong Island, Coll. J. C. F. Chan.

Diagnosis. *Parazacco ignis* sp. nov. can be distinguished from *P. spilurus* by the following combination of features in specimens > 50 mm SL: shorter caudal peduncle length (15.1 – 18.8% SL vs 16.0 – 19.5); shorter upper jaw length (38.2 – 43.9% HL vs 41.4 – 46.5); fewer lateral line scales (mode 43 vs mode 46); fewer pre-dorsal scales (mode 20 vs mode 22); fewer tubercules on the lower jaw extending to the lower cheek with the first and last tubercules being significantly larger (mode 2 vs mode 4 and evenly sized tubercules); top of head is less compressed (vs more compressed; Fig. 7); black lateral stripe appears to be blotchy in juveniles (vs more solid; Fig. 8); and red-orange coloration of the chin extending to the belly in specimens < 80 mm SL (vs no coloration to minimal red-orange specks; see Fig. 6). *Parazacco ignis* sp. nov. can be distinguished from *P. fasciatus* by having a shorter head (22.1 – 24.6% TL vs 28) with the top being the least compressed (vs the most compressed of the three species; Fig. 7), slimmer body (17.0 –21.8% TL vs 25), shorter snout (27.8 – 35.5% HL vs 35.7 – 43.4), and more pelvic fin rays (7 – 9 vs 6) (Koller, 1927; Ito and Hosoya, 2016). A full comparison of morphometric and meristic data among the three species is given in Table 2. Measurements of the holotype and paratypes are provided in Table 4.

Figure 8. Comparisons of full lateral body of: **(A)** *Parazacco spilurus* juvenile 49.0 mm SL, Hong Kong, New Territories, Ma Wo; **(B)** *P. spilurus* juvenile 29.4 mm SL, Hong Kong, New Territories, Ma Wo; **(C)** *P. ignis* sp. nov. juvenile 51.1 mm SL, Hong Kong, New Territories, Sam A Chung; **(D)** *P. ignis* sp. nov. juvenile 32.9 mm SL, Hong Kong, New Territories, Sam A Chung.

Description. Morphometric data is given in Tables 2 and 4. Meristic data are as follows: 7 dorsal fin rays; 11 (7) – 12 (8) anal fin rays; 13 (11) – 14 (4) pectoral fin rays; 7 (7), 8 (6), or 9 (2) pelvic fin rays; 9 + 8 caudal fin rays; 40 (2), 41 (3), 42 (1), 43 (4), 44 (3), or 45 (2) lateral line scales; 8 (3) – 9 (12) scales above lateral line; 2 (1), 3 (11), or 4 (3) scales below lateral line; 19 (1), 20 (7),

21 (5), 22 (2) pre-dorsal scales; 7 (1), 8 (13), or 9 (1) caudal peduncle scales; 1 (1), 2 (3), 3 (1), 4 (3), 5 (1), 6 (1), 7 (3), or 9 (2) tubercles on lower jaw and cheek; 20 – 22 + 19 – 21 = 41 (5), 42 (10), 43 (6) vertebrae.

General body form as in Fig. 6E – H. Body elongate and laterally compressed. Head somewhat depressed. No maxillary barbels. Eyes rather large. Upper lip notched with prominent front edge of lower jaw. Tubercles distinct on head and present in all specimens < 50 mm SL, with a single row of 1 – 9 tubercles on lower jaw that extends just before the opercle; tubercles also present on snout and as a row above the upper lip extending to under the eyes before the opercle. Body with cycloid scales and complete lateral line, which abruptly runs downward just above the pectoral fin and extends into middle of caudal fin base. Supra-pectoral and supra-pelvic flaps present.

When alive, light to dark grey starting from the lower lip, through the snout and dorsal body, gradually turning white on the lateral sides below the lateral line. A black horizontal stripe runs above the lateral line from the gills to the caudal peduncle and is most prominent in juveniles before fading from anterior to posterior among larger the specimen. Black vertical stripe on operculum and black spot on caudal peduncle, which is also most prominent in juveniles before fading with maturation. All fins pale yellow and become increasingly vibrant with increasing size. Red-orange coloration develops in dorsal and anal fins and under the chin and belly of specimens > 80 mm SL.

When preserved, head and dorsal body retains light grey and becomes paler on the lateral side below the lateral line. Black spot on caudal peduncle becomes more apparent. Fins lose yellow and red coloration, but dark oblong bands between dorsal fin rays remain.

Comparative material. *Parazacco spilurus*: BMNH 1956.2.25.1–5 (5 syntypes; X-rays from BMNH Data portal; data and pictures from Ito and Hosoya (2016)); ZRC 68029, 99.2 mm SL, Ma Wo, foothills of Tai Mo Shan, central New Territories, Coll. J. C. F. Chan and B. W. Low; ZRC 68034, 4 ex., 50.9–122.1 mm SL, Yung Shue O, New Territories, Coll. J. C. F. Chan; ZRC 68033, 4 ex., 69.6–81.0 mm SL, San Tau, Lantau Island, Coll. J. C. F. Chan; ZRC 68035, 5 ex., 77.7 – 108.0 mm SL, Shui Hau, Lantau Island, Coll. J. C. F. Chan; ZRC 68032, 7 ex., 16.5 – 82.2 mm SL, Tai Tan, New Territories, Coll. J. C. F. Chan; ZRC 68030, 2 ex., 29.4 – 49.0 mm SL, Ma Wo, New Territories, Coll. J. C. F. Chan and B. W. Low. *Parazacco fasciatus*: X-ray and pictures of holotype and 12 syntypes from A. Palandačić, NMW; data on the same specimens from Koller (1927) and Ito and Hosoya (2016).

Habitat. So far only known from low elevation coastal streams (< 100m above sea level) or former coastal streams (Plover Cove Reservoir is < 100m from sea).

Distribution. From the present study, it is known from four sites in the eastern New Territories (Sam A Chung, Plover Cove Reservoir, Hoi Ha, and Lai Chi Chong) and one site on Hong Kong Island (Tai Tam), Hong Kong (Fig. 1). It is also recorded in Kai Ku Shue Ha (Wu et al., 2019).

Etymology. The species epithet is derived from the Latin words *ignis*, which mean fiery red. The species is named in reference to the red-orange coloration found on its throat and belly of mature male fish.

Discussion

Species boundaries, cryptic speciation, and hybridisation

The present study confirms the presence of an independent lineage previously misidentified as *Parazacco spilurus* in Hong Kong, supporting earlier findings on mitochondrial CR and cyt b sequences (Wu, 2017; Wu et al., 2019). A congruence of conclusive evidence is observed from the integrated approach of genomic and morphomeristic analyses. The divergence period of *P. spilurus* and *P. ignis* sp. nov. (~4.87 mya) is less than the coalescence time to the genus *Opsariicthys* (when *Opsariicthys* was split into two major phylogroups (*O. bidens* and *O. evolans*-related species) ~6.43 mya; Lin et al., 2016) but exceeds both phylogroups interspecies divergence range (~4.15 – 1.88 mya; Lin et al., 2016). Diagnostic characters are identified and provide further evidence that those lineages represent a separate cryptic species. Our integrative approach provides conclusive evidence that there are two independent lineages of *Parazacco* in Hong Kong. *Parazacco spilurus* is widely distributed around the region except the northeastern-most part of the New Territories in Hong Kong, whereas *P. ignis* sp. nov. is restricted to the northeastern part of New Territories with a single population in southern Hong Kong Island.

With the exception of the widely distributed *Opsariichthys bidens* and *Zacco platypus* across China and East Asia respectively, other species in the opsariicthine group are restricted to smaller areas such as river basins (Peng et al., 2024). Revisions of the group have resulted in the revalidation (e.g., *O.amurensis* Berg 1932, *O.hainanensis* Nichols and Pope, 1927) and description (e.g., *O. iridescens* Peng, Zhou and Yang, 2024) of several species (Wang et al., 2019). Our findings in Hong Kong support this and show that the range of *P. spilurus* is more restricted than previously believed. The case may be similar with *P. fasciatus* (type locality in Hainan Island, China), which has several names synonymised from the Thia River (as *Opsariichthys elegans* Pellegrin and Chevey, 1934); Ban Can stream (as *Parazacco babeensis* Nguyen and Nguyen, in Nguyen and Nguyen, 2000; as *Parazacco vinhi* Nguyen and Nguyen, in Nguyen and Nguyen, 2000); and Vu Quang Mountain (as *Parazacco vuquangensis* Nguyen, 1995) in northern and central Vietnam. Earlier molecular analyses by Wu (2017) showed three distinct lineages of *Parazacco* that correspond to three putative species (*P. spilurus*, *P. fasicatus*, *P.* sp.), which are supported in our morphological analyses. Future work on the genus will likely require the integrative taxonomic assessment of fresh material across its entire range to reassess species boundaries and resolve species identities.

Our analyses identified two hybrids in one locality, corresponding to the low levels of hybridisation reported by Wu et al. (2019) and suggests incipient speciation. Hybridisation among young species has been recently found to be more common than previously believed (Irisarri et al. 2018) and records of hybridisation between species in the opsariicthine group are also common (O. platypus x Zacco platypus (Wang et al., 1997); O. evolans.x Z. platypus (Liao et al., 2020)). However, detection within species complexes may be more difficult despite being a relatively widespread phenomenon (Nolte and Tautz, 2010). Our yardstick approach suggests that divergence is comparable to other species pairs in the opsariichthine group and shows that an integrative taxonomic approach may be necessary for discerning these hybrids.

The hybrids were found in Lai Chi Chong and adjacent sites (~ 2km south, Yung Shue O, *P. spilurus*; ~ 100m east, Hoi Ha, *P. ignis* sp. nov.) only contained pure populations of either species, indicating Lai Chi Chong is likely a natural contact zone. While Wu et al. (2019) did not cover Lai

Chi Chong, they reported hybrids in the Plover Cove Reservoir area. Although we also encountered both species, we did not record hybrids at Plover Cove Reservoir and suggests hybridization rates may be low. A third contact zone, Tai Tam Tuk Reservoir is also identified in Wu et al. (2019), but we did not encounter any *Parazacco* spp. likely due to high water levels at the time of sampling. The ecological and genetics impacts of these contact zones have yet to be explored, although we concur with Wu et al. (2019) that inter-reservoir water transfers or intentional release of fish may lead to the artificial mixing of species and creation of hybrids. A major consequence of hybridization may be the loss of co-adapted gene complexes and local adaptations (Barton and Hewitt, 1989). For instance, low levels of human-mediated hybridisation have been known to markedly reduce reproductive success of *Oncorhynchus mykiss* Walbaum, 1792 and *Oncorhynchus clarkii lewisi* Richardson, 1836 (Muhlfeld et al., 2009). Furthermore, the genetic diversity of *P. ignis* sp. nov. has shown to be consistently low at both the mitochondrial (Wu et al., 2019) and genomic level. Given the restricted distribution and fewer known populations of *P. ignis* sp. nov., maintenance of the genetic integrity of remaining populations should be made a conservation priority to prevent impacts on fitness and genomic extinction (Epifanio and Philipp, 2000).

Biogeography

Our ddRADseq sequencing showed that *P. spilurus* and *P. ignis* sp. nov. diverged during the early Pliocene (~4.87 mya). This period was characterized with major major sea-level transgressions ~150m above sea level, which separated Hong Kong Island and Lantau Island from the mainland (i.e., New Territories) for prolonged periods (Fyfe et al., 2000; Ding et al., 2013). Sea levels subsequently fluctuated throughout the late Pleistocene (0.126 – 0.0177 mya) with the South China Sea plummeting to ~130 meters below present during the late Quaternary glacial stages (Wang and Li, 2009). This may have reconnected previously isolated streams among Hong Kong Island, Lantau Island, and the New Territories and allowed geneflow, potentially explaining why there is no clear paleodrainage association between the two species, yet some within-species trends were present, e.g., the Lantau Island lineage is the most divergent within *P. spilurus*, which is consistent with the island's period of separation. This hypothesised biogeographical history for *Parazacco* species also align with speciation and population differentiation of other freshwater fauna in Hong Kong between the late Miocene to early Pliocene: speciation of *Caridina logemmani* from *C. cantonensis* (~4.2 mya) and their subsequent secondary contact and hybridisation (Chow et al., 2021); and population differentiation within *Schistura fasciolata and Pseudeogastromyzon myersi* (Wong et al., 2017).

Suppression of Parazacco spilurus syntypes and neotype designation

The inclusion of morphomeristic analyses into prior phylogenetic studies of *Parazacco spilurus* have been limited by the damaged and bleached state of the syntypes, comprising juvenile specimens (Ito and Hosoya, 2016; Wu, 2017). The poor condition and potential influence of allometric growth on the syntypes will greatly affect the accuracy of morphomeristic counts and ratios, although the lateral line scale counts (46) reported in Günther (1868) matches those of this study (mode 46; but see Ito and Hosoya, 2016). The issue is compounded by the vague description of the type locality being from "inland mountainous regions of Hong Kong" (Günther, 1868). This is inferred to be in any part of Hong Kong Island or southern Kowloon, as the species description was prior the cession of the New Territories into the Hong Kong territory (1898; Historical Laws of Hong Kong Online, 2025). Presently, the entirety of southern Kowloon (south Boundary Street

onwards) is now developed, while only small mountain streams and reservoirs remain on Hong Kong Island. It is possible the type locality of *P. spilurus* no longer exists due to development or is contaminated with translocations via water transfers in reservoirs (e.g., presence of both *P. spilurus* and *P. ignis* sp. nov. in Tai Tam Tuk Reservoir, Hong Kong Island; Wu et al., 2019).

Article 75.5 of the International Code of Zoological Nomenclature (ICZN) states that if "the taxonomic identity of a nominal species-group taxon cannot be determined from its existing name-bearing type (i.e., its name is a nomen dubium), and stability or universality are threatened thereby, the author may request the Commission to set aside under its plenary power [Art. 81] the existing name-bearing type and designate a neotype." (ICZN, 1999). Therefore, we propose for a suppression of the type material and designation of a neotype with an adult specimen under Article 75.5 of the ICZN (case to be submitted to the Bulletin of Zoological Nomenclature upon acceptance of this article; ICZN, 1999). Given the absence of habitat in Kowloon and habitat degradation and presence of both species in Hong Kong Island, the proposed neotype was collected from a pure population in Ma Wo, central New Territories. Only *P. spilurus* occurs in the neotype locality and its adjacent drainages (Lam Tsuen River and Tai Po Kau), which ensures stability in its taxonomy.

Conclusion

The present study delineates the species boundaries of *P. spilurus* in Hong Kong using an integrative taxonomic approach and the presence of a cryptic species is verified and described. A natural hybrid population was uncovered along with two additional contact zones in reservoirs but reproductive isolation is maintained, and the overall hybridisation is low. Nonetheless, hybrids likely occur in reservoirs, and more research is needed to assess how hybridisation in reservoir populations affect their ecology and genetics. Work on how reproductive isolation is maintained and conservation measures to prevent further human-mediated hybridisation is also recommended. This study also recommends the suppression of the syntypes of *P. spilurus* and a neotype is designated to stabilize the taxonomy of the species, which will become the basis for comparisons across the opsariichthine group. The revaluation of the genus *Parazacco* across its entire geographic range is urgently needed to validate species identities, delineate species distributions, and describe potential cryptic species from this species complex.

Acknowledgements

We thank Alex Lau, Yip Hon Tim, Yui Hong Chiu, Samuel C. L. Ho, and Sandy S. M. Yau for assistance with fieldwork; we thank Anja Palandačić at Naturhistorisches Museum Wien for providing photographs and X-rays of the *Parazacco fasciatus* types; we thank Anthony Lau, Jessie Lai, Kelvin Lim, for assistance in curation of specimens; the Lee Kong Chian Natural History Museum, and the National University of Singapore for providing technical support.

Funding

This work was partially funded by the Environmental Conservation Fund (ECF 52/2020).

Supporting information

Table S1. Summary statistics of *Parazacco* species in each locality using genome-wide SNPs.
AR: allelic richness; H_O: observed heterozygosity; H_E: expected heterozygosity; n: sample size.

Figure S1. Hybrid detection accuracy was assessed through three independent simulations with three replicates each. Simulated multigenerational hybrids were created using the top 100, 200, and 300 SNPs with the highest F_{ST} and no linkage disequilibrium. Coloured lines represent hybrid detection power at various probability thresholds: P1= pure *Parazacco spilurus*; P2= pure *P. ignis* sp. nov.; F1= first-generation hybrids; F2= second-generation hybrids; BC1= backcross of hybrid to pure *P. spilurus*; BC2= backcross of hybrid to pure P. *ignis* sp. nov.

Figure S2. Hybrid detection efficiency was assessed through three independent simulations with three replicates each. Simulated multigenerational hybrids were created using the top 100, 200, and 300 SNPs with the highest F_{ST} and no linkage disequilibrium. Coloured lines represent hybrid detection power at various probability thresholds: P1= pure *Parazacco spilurus*; P2= pure *P. ignis* sp. nov.; F1= first-generation hybrids; F2= second-generation hybrids; BC1= backcross of hybrid to pure *P. spilurus*; BC2= backcross of hybrid to pure P. *ignis* sp. nov.

Conflict of interest

The authors declare no conflict of interest.

Data availability statement

All aligned sequences (BAM format) from the present study are deposited in the Sequence Read Archive under the BioProject accession PRJNA1290245.

References

AFCD (2025) Hong Kong Biodiversity Information Hub - Species Database. Available at: https://bih.gov.hk/en/species-database/index.html. Accessed June 23 2025.

Armbruster JW (2012) Standardized measurements, landmarks, and meristic counts for cypriniform fishes, Zootaxa 3586: 8–16. https://doi.org/10.11646/zootaxa.3586.1.3

Barton NH, Hewitt GM (1989) Adaptation, speciation and hybrid zones, Nature 341: 497–503. https://doi.org/10.1038/341497a0

Bryant D, Bouckaert R, Felsenstein J, Rosenberg N, RoyChoudhury A (2012) Inferring species trees directly from biallelic genetic markers: bypassing gene trees in a full coalescent analysis, Molecular Biology and Evolution 29:1917–32. https://doi.org/10.1093/molbev/mss086

Chan EKW, Zhang Y, Dudgeon D (2008) Arthropod 'rain'into tropical streams: the importance of intact riparian forest and influences on fish diets, Marine and Freshwater Research 59: 653–60. https://doi.org/10.1071/MF07191

Chan JCF, Liew JH, Dudgeon D (2024) High spatial variability in a species-rich assemblage of diadromous fishes in Hong Kong, Southern China, Journal of Fish Biology 105: 663–81. https://doi.org/10.1111/jfb.15812

Cheng P, Yu D, Tang Q, Yang J, Chen Y, Liu H (2022) Macro-evolutionary patterns of East Asian opsariichthyin-xenocyprinin-cultrin fishes related to the formation of river and river-lake environments under monsoon climate, Water Biology and Security *1*: 100036. https://doi.org/10.1016/j.watbs.2022.100036

Chong D and Dudgeon D (1992) Hong Kong stream fishes: an annotated checklist with remarks on conservation status, Memoirs of the Hong Kong Natural History Society 19: 79–112.

Chow LH, Tsang LM, Chu KH, Ma KY (2022) Genetic assessment of the rare freshwater shrimp *Caridina logemanni* endemic to Hong Kong and its hybridisation with a widespread congener, Marine and Freshwater Research 73: 491–502. https://doi.org/10.1071/MF21192

Ding W, Li J, Li J, Fang Y, Tang Y (2013) Morphotectonics and evolutionary controls on the Pearl River canyon system, South China Sea, Marine Geophysical Research 34: 221–38. https://doi.org/10.1007/s11001-013-9173-9

Drummond AJ, Rambaut A (2007) BEAST: Bayesian evolutionary analysis by sampling trees, BMC Evolutionary Biology 7: 214. https://doi.org/10.1186/1471-2148-7-214

Epifanio J, Philipp D (2000) Simulating the extinction of parental lineages from introgressive hybridization: the effects of fitness, initial proportions of parental taxa, and mate choice, Reviews in Fish Biology and Fisheries 10: 339–54. https://doi.org/10.1023/A:1016673331459

650 Evanno G, Regnaut S, Goudet J (2005) Detecting the number of clusters of individuals using the
651 software STRUCTURE: a simulation study, Molecular Ecology 14: 2611–20.
652 https://doi.org/10.1111/j.1365-294x.2005.02553.x

653 Fyfe J, Shaw R, Campbell S, Lai KW, Kirk PA (2000) The quaternary geology of Hong Kong.
654 Geotechnical Engineering Office, Civil Engineering Department, Government of Hong Kong,
655 Hong Kong.

656 Günther A (1868) Catalogue of the Physostomi, containing the families Heteropygii, Cyprinidæ,
657 Gonorhynchiidæ, Hypodontidæ, Osteoglossidæ, Clupeidæ, Chirocentridæ, Alepochephalidæ,
658 Notopteridæ, Halosauridæ, in the collection of the British Museum, Catalogue of Fishes 7: 1–
659 512.

660 Helfrich P, Rieb E, Abrami G, Lücking A, Mehler A (2018) TreeAnnotator: versatile visual
661 annotation of hierarchical text relations, Proceedings of the eleventh international conference on
662 language resources and evaluation (LREC 2018) 1958–63.

663 Historical Laws of Hong Kong Online (2025) NEW TERRITORIES (REGULATION)
664 ORDINANCE, 1899. Available at: https://oelawhk.lib.hku.hk/items/show/721. Accessed June 10
665 2025.

666 Hubbs CL, Lagler KF (2004) Fishes of the Great Lakes region, revised edition. University of
667 Michigan Press, Michigan.

668 ICZN (1999) International Commission on Zoological Nomenclature (Fourth Edition). The
669 International Trust for Zoological Nomenclature, London.

670 Irisarri I, Singh P, Koblmuller S, Torres-Dowdall J, Henning F, Franchini P, Fischer C, Lemmon
671 AR, Lemmon EM, Thallinger GG, Sturmbauer C, Meyer A (2018) Phylogenomics uncovers
672 early hybridization and adaptive loci shaping the radiation of Lake Tanganyika cichlid
673 fishes, Nature Communications 9: 3159. https://doi.org/10.1038/s41467-018-05479-9

674 Ito T, Hosoya K (2016) Re-examination of the type series of *Parazacco spilurus* (Teleostei:
675 Cyprinidae), FishTaxa-Journal of Fish Taxonomy 1:89–93.
676 https://doi.org/10.7508/fishtaxa.2016.02.004

677 Jiang Z, Jiang J, Wang Y, Zhang E, Zhang Y, Li L, Xie F, Cai B, Cao L, Zheng G, Dong L,
678 Zhang Z, Ding P, Luo Z, Ding C, Ma Z, Tang S, Cao W, Li C, Hu H, Ma Y, Wu Y, Wang Y,
679 Zhou K, Liu S, Chen Y, Li J, Feng Z, Wang Y, Wang B, Li C, Song X, Cai L, Zang C, Zeng Y,
680 Z Meng, Fang H, Ping X (2016) Red list of China's vertebrates, Biodiversity Science 24: 500–
681 551. https://doi.org/10.17520/biods.2016076

682 Koller O (1927) Fische von der Insel Hai-nan, Annalen des Naturhistorischen Museums in Wien
683 41: 25–49.

Kopelman NM, Mayzel J, Jakobsson M, Rosenberg NA, Mayrose I (2015) Clumpak: a program for identifying clustering modes and packaging population structure inferences across K, Molecular Ecology Resources 15: 1179–91. https://doi.org/10.1111/1755-0998.12387

Kottelat M (2001) Freshwater fishes of northern Vietnam: a preliminary check-list of the fishes known or expected to occur in northern Vietnam with comments on systematics and nomenclature. Washington: Environment and Social Development Unit, East Asia and Pacific Region, The World Bank,.

Kottelat M (2013) The fishes of the inland waters of Southeast Asia : a catalogue and core bibliography of the fishes known to occur in freshwaters, mangroves and estuaries, Raffles Bulletin of Zoology, 27: 1–663.

Lau DC, Leung KM, Dudgeon D (2009) What does stable isotope analysis reveal about trophic relationships and the relative importance of allochthonous and autochthonous resources in tropical streams? A synthetic study from Hong Kong, Freshwater Biology 54: 127–41. https://doi.org/10.1111/j.1365-2427.2008.02099.x

Lee LF, Lam KS, Ng KY, Chan KT, Young LC (2004) Field Guide to the Freshwater Fish of Hong Kong. Agriculture, Fisheries and Conservation Department, Friends of the Country Parks and Cosmos Books Ltd, Hong Kong.

Li H, Durbin R (2009) Fast and accurate short read alignment with Burrows-Wheeler transform, Bioinformatics 25: 1754–60. https://doi.org/10.1093/bioinformatics/btp324

Li H, Handsaker B, Wysoker A, Fennell T, Ruan J, Homer N, Marth G, Abecasis G, Durbin R (2009) The Sequence Alignment/Map format and SAMtools, Bioinformatics *25*: 2078–79. https://doi.org/10.1093/bioinformatics/btp352

Li H, Wei Z, Chang H (2003) The diagnosis and distribution of *Parazacco spilurus*, Journal of Xinyang Normal University (Natural Science Edition) 16: 307–08.

Liao NL, Huang SP, Wang TY (2020) Interspecific mating behavior between introduced *Zacco platypus* and native *Opsariichthys evolans* in Taiwan, Zoological Studies 59: e6. https://doi.org/10.6620/ZS.2020.59-6

Lin H-D, Kuo P-H, Wang W-K, Chiu Y-W, Ju Y-M, Lin F-J, Hsu K-C (2016) Speciation and differentiation of the genus *Opsariichthys* (Teleostei: Cyprinidae) in East Asia, Biochemical Systematics and Ecology 68: 92–100. https://doi.org/10.1016/j.bse.2016.07.001

Liu D, Gui L, Zhu Y, Xu C, Zhou W, Li M (2022) Chromosome-level assembly of male *Opsariichthys bidens* genome provides insights into the regulation of the GnRH signaling pathway and genome Evolution, Biology 11: 1500. https://doi.org/10.3390/biology11101500

717 Malinsky M, Trucchi E, Lawson DJ, Falush D (2018) RADpainter and fineRADstructure:
718 population inference from RADseq data, Molecular Biology and Evolution 35: 1284–90.
719 https://doi.org/10.1093/molbev/msy023

720 Man SH, Hodgkiss IJ (1981) Hong Kong Freshwater Fishes. Urban Council, Wishing Printing
721 Company, Hong Kong.

722 Muhlfeld CC, Kalinowski ST, McMahon TE, Taper ML, Painter S, Leary RF, Allendorf FW
723 (2009) Hybridization rapidly reduces fitness of a native trout in the wild, Biology Letters 5: 328–
724 31. https://doi.org/10.1098/rsbl.2009.0033

725 Nolte AW, Tautz D (2010) Understanding the onset of hybrid speciation, Trends in Genetics, 26:
726 54–8. https://doi.org/10.1016/j.tig.2009.12.001

727 Osse JWM, Boogaart JGM (1995) Fish larvae, development, allometric growth, and the aquatic
728 environment, ICES Marine Science Symposium 201: 21–34.
729 https://doi.org/10.17895/ices.pub.19271519

730 Pan JH, Zhong L, Wu HL, Zheng CY, Liu JZ, Ye FL, Chen XL, Kuang YD, Lin DQ, Gao GF,
731 Liu CH & Lu KX (1991) The freshwater fishes of Guangdong Province. Guangdong Science and
732 Technology Press, Guangzhou.

733 Paris JR, Stevens JR, Catchen JM (2017) Lost in parameter space: a road map for
734 stacks, Methods in Ecology and Evolution 8; 1360–73. https://doi.org/10.1111/2041-210X.12775

735 Peng X, Zhou J-J, Gao H-D, Yang J-Q (2024) A new species of *Opsariichthys* (Teleostei,
736 Cypriniformes, Xenocyprididae) from Southeast China, Zookeys 1214: 15–34.
737 https://doi.org/10.3897/zookeys.1214.127532

738 Peterson BK, Weber JN, Kay EH, Fisher HS, Hoekstra HE (2017) Double digest RADseq: an
739 inexpensive method for de novo SNP discovery and genotyping in model and non-model
740 species, PLoS One 7: e37135. https://doi.org/10.1371/journal.pone.0037135

741 Pritchard JK, Stephens M, Donnelly P (2000) Inference of population structure using multilocus
742 genotype data, Genetics 155: 945–59. https://doi.org/10.1093/genetics/155.2.945

743 Purcell S, Neale B, Todd-Brown K, Thomas L, Ferreira MAR, Bender D, Maller J, Sklar P, de
744 Bakker PIW, Daly MJ, Sham PC (2007) PLINK: a tool set for whole-genome association and
745 population-based linkage analyses, The American Journal of Human Genetics 8: 559–75.
746 https://doi.org/10.1086/519795

747 Underwood W, Anthony R (2020) AVMA guidelines for the euthanasia of animals: 2020
748 edition. Available at: https://www.avma.org/sites/default/files/2020-02/Guidelines-on-
749 Euthanasia-2020.pdf. Accessed May 2 2025.

R Core Team (2024) *R: A language and environment for statistical computing*. Vienna: R Foundation for Statistical Computing. Available at: https://www.R-project.org/. Accessed September 2024.

Rambaut A (2016) FigTree v1.4.3. Available at: https://github.com/rambaut/figtree/releases/tag/v1.4.3. Accessed October 3 2025.

Roberts TR (1989) The Freshwater Fishes of Western Borneo (Kalimantan Barat, Indonesia), Memoirs of the California Academy of Sciences 14: 1–210.

Rochette NC, Rivera-Colon AG, Catchen JM (2019) Stacks 2: Analytical methods for paired-end sequencing improve RADseq-based population genomics, Molecular Ecology 28: 4737–54. https://doi.org/10.1111/mec.15253

Tsang AHF, Dudgeon D (2021) Do exotic poeciliids affect the distribution or trophic niche of native fishes? Absence of evidence from Hong Kong streams, Freshwater Biology 66: 1751–64. https://doi.org/10.1111/fwb.13789

Vähä JP, Primmer CR (2006) Efficiency of model-based Bayesian methods for detecting hybrid individuals under different hybridization scenarios and with different numbers of loci, Molecular Ecology 15: 63–72. https://doi.org/10.1111/j.1365-294x.2005.02773.x

Wang S (1998) China Red Data Book of Endangered Animals: Pisces. National Environmental Protection Agency, China.

Wang HY, Lee SC, Yu MJ (1997) Genetic evidence to clarify the systematic status of the genera *Zacco* and *Candidia* (Cypriniformes: Cyprinidae), Zoological Studies 36: 170–77.

Wang PX, Li QY (2009) The South China Sea: Paleoceanography and Sedimentology. Springer Dordrecht, Netherlands.

Wang X, Liu F, Yu D, Liu H (2019) Mitochondrial divergence suggests unexpected high species diversity in the opsariichthine fishes (Teleostei: Cyprinidae) and the revalidation of *Opsariichthys macrolepis*, Ecology and Evolution 9: 2664–77. https://doi.org/10.1002/ece3.4933

Wong WY, Ma KY, Tsang LM, Chu KH (2017) Genetic legacy of tertiary climatic change: a case study of two freshwater loaches, *Schistura fasciolata and Pseudogastromyzon myersi*, in Hong Kong. Heredity 119: 360–70. https://doi.org/10.1038/hdy.2017.47

Wringe BF, Stanley RRE, Jeffery NW, Anderson EC, Bradbury IR (2017a) hybriddetective: A workflow and package to facilitate the detection of hybridization using genomic data in R, Molecular Ecology Resources 17: e275–e84. https://doi.org/10.1111/1755-0998.12704

Wringe BF, Stanley RR, Jeffery NW, Anderson EC, Bradbury IR (2017b) parallelnewhybrid: an R package for the parallelization of hybrid detection using newhybrids, Molecular Ecology Resources 17: 91–95. https://doi.org/10.1111/1755-0998.12597

784 Wu TH (2017) Population genetics of four common indigenous fish species in Hong Kong
785 streams. D. Phil. Thesis, Chinese University of Hong Kong.
786 (https://repository.lib.cuhk.edu.hk/en/item/cuhk-1839476).

787 Wu TH, Tsang LM, Chow LH, Chen I-S, Chu KH (2019) Cryptic lineages and hybridization of
788 the predaceous chub *Parazacco spilurus* (Actinopterygii, Cypriniformes, Xenocyprididae) in
789 Hong Kong, Hydrobiologia 826: 99–111. https://doi.org/10.1007/s10750-018-3720-y

790 Zheng X, Levine D, Shen J, Gogarten SM, Laurie C, Weir BS (2012) A high-performance
791 computing toolset for relatedness and principal component analysis of SNP data, Bioinformatics
792 28: 3326–8. https://doi.org/10.1093/bioinformatics/bts606

Tables

Table 1. Species, specimens and localities of material used for genetic and morphomeristic analyses. Specimens examined are housed in the Lee Kong Chian Natural History Museum, Zoological Reference Collection (ZRC), National University of Singapore, Singapore; Lingnan Natural History Collection (LINGU-FISH), Lingnan University, Hong Kong, China; Natural History Museum (BMNH), London, United Kingdom; and Naturhistorisches Museum Wien (NMW), Vienna, Austria; * denotes populations used for phylogenomic analyses.

Catalogue no.	**Species**	**Locality**	**Abbreviation**	**No. specimens for genetic analysis**	**No. specimens for morphomeristics**	**Remarks**
BMNH 1956.2.25.1-5	*Aspius spilurus*	Inland mountainous regions of Hong Kong	-	-	5	Syntypes; X-rays from NHM data portal
LINGU-FISH-00045	*Parazacco spilurus*	Lam Tsuen River, New Territories, Hong Kong, China	LT	10*	-	
ZRC 68029	*Parazacco spilurus*	Ma Wo, New Territories, Hong Kong, China	MW	-	1	Proposed neotype
ZRC 68030	*Parazacco spilurus*	Ma Wo, New Territories, Hong Kong, China	MW	-	2	
LINGU-FISH-00041	*Parazacco spilurus*	Ma Wo, New Territories, Hong Kong, China	MW	10*	-	
LINGU-FISH-00110	*Parazacco spilurus*	Tai Po Kau, New Territories,	TPK	10*	-	

		Hong Kong, China				
ZRC 68032	*Parazacco spilurus*	Tai Tan, New Territories, Hong Kong, China	TT	5	4	
ZRC 68034	*Parazacco spilurus*	Yung Shue O, New Territories, Hong Kong, China	YSO	5*	4	
ZRC 68033	*Parazacco spilurus*	San Tau, Lantau Island, Hong Kong, China	ST	-	4	
ZRC 68035	*Parazacco spilurus*	Shui Hau, Lantau Island, Hong Kong, China	SH	5*	5	
ZRC 68031	*Parazacco spilurus*	Wong Lung Hang, Lantau Island, Hong Kong, China	WLH	5*	-	
LINGU-FISH-00095	*Parazacco* spp.	Plover Cove Reservoir, New Territories, Hong Kong, China	PC	13	-	Both species occur; all juveniles
ZRC 68040 – 68041	*Parazacco* spp.	Lai Chi Chong, New Territories, Hong Kong, China	LCC	5	-	Both species and hybrids occur here; all juveniles
ZRC 68039	*Parazacco ignis* sp. nov.	Hoi Ha, New Territories,	HH	5*	6	Paratypes

		Hong Kong, China				
ZRC 68036	*Parazacco ignis* sp. nov.	Sam A Chung, New Territories, Hong Kong, China	SAC	-	1	Holotype
ZRC 68037	*Parazacco ignis* sp. nov.	Sam A Chung, New Territories, Hong Kong, China	SAC	5*	10	Paratypes
ZRC 68038	*Parazacco ignis* sp. nov.	Chai Tai stream, Tai Tam, Hong Kong Island, Hong Kong, China	CT	10*	5	Paratypes
NMW10407 – 10419	*Parazacco fasciatus*	Kang-Kong River, Hainan Island, China	-	-	13	Holotype and 12 paratypes; X-rays and pictures from NMW; note 14 were reported in Koller (1927) but only 13 in collection
Uncatalogued	*Acrossocheilus beijiangensis*	Lantau Island, Hong Kong, China	-	2*	-	Outgroups
LINGU-FISH-00134	*Acrossocheilus parallens*	New Territories, Hong Kong, China	-	1*	-	Outgroups
LINGU-FISH-00090	*Opsariichthys evolans*	New Territories, Hong Kong, China	-	2*	-	Outgroups

LINGU-FISH-00052	*Opsariichthys bidens*	New Territories, Hong Kong, China	-	1*	-	Outgroups

799

Table 2. Morphomeristic and meristic data for *Parazacco ignis*, *P. spilurus* and *P. fasciatus*. Numbers in parentheses indicate the mean for morphometric data and mode for meristic data; *Based on morphometrics provided in Koller (1927) and translated morphometrics of Koller (1927) in Ito and Hosoya (2016); #based on counts of X-rays of the holotype and paratypes of P. fasciatus provided by the Natural History Museum Vienna (note that caudal fin counts were conducted on eight specimens due to damaged and warped fins).

	Parazacco ignis (n=22)	*P. spilurus* (n=16)	*P. fasciatus* (n=13)
Total length (mm TL)	64.3 – 118.7 (91.3)	62.8 – 140.6 (101.7)	90 – 140*
Standard length (mm SL)	51.4 – 96.5 (74.3)	50.9 – 122.9 (84.2)	–
Morphometric data			
% TL			
Head length	22.1 – 24.6 (23.6)	20.3 – 26.5 (23.0)	28*
Body depth	17.0 – 21.8 (19.1)	17.3 – 22.6 (19.9)	25*
% SL			
Head length	27.6 – 30.9 (29.1)	24.1 – 30.2 (27.8)	–
Body depth	21.2 – 25.7 (23.5)	21.0 – 26.9 (24.0)	–
Body width at dorsal origin	7.2 – 11.4 (9.1)	7.1 – 11.8 (8.9)	–
Body width at anal origin	5.0 – 8.7 (6.9)	5.7 – 10.0 (6.9)	–
Caudal peduncle depth	9.3 – 10.8 (10.0)	9.2 – 10.9 (9.8)	–
Caudal peduncle length	15.1 – 18.8 (16.8)	16.0 – 19.5 (18.1)	–
Pre-dorsal	52.2 – 55.1 (53.5)	51.1 – 54.3 (52.8)	–
Pre-anal	65.1 – 70.6 (67.5)	64.4 – 68.1 (66.4)	–
Dorsal origin to caudal base	41.4 – 48.5 (45.1)	43.5 – 49.1 (46.4)	–
Pectoral origin to pelvic insertion	22.5 – 26.9 (24.6)	24.2 – 27.5 (25.4)	–
Longest dorsal ray	17.1 – 24.3 (20.7)	17.1 – 21.4 (19.1)	–
Longest anal ray	19.3 – 34.7 (24.9)	17.8 – 34.9 (25.3)	–
Longest pectoral ray	18.5 – 22.4 (20.7)	15.6 – 22.3 (20.0)	–
Dorsal fin base	10.0 – 13.1 (11.5)	10.0 – 13.2 (11.3)	–
Anal fin base	13.6 – 16.4 (14.9)	12.1 – 16.3 (14.9)	–
Longest Pelvic fin ray	13.9 – 18.3 (16.1)	11.6 – 16.9 (15.4)	–
% HL			
Head width at nasal section	17.0 – 22.3 (19.7)	17.6 – 21.5 (20.0)	–
Snout length	27.8 – 35.5 (31.7)	28.7 – 36.0 (32.4)	35.7 – 43.4*
Inter-orbital width	29.0 – 33.8 (31.5)	29.2 – 36.3 (32.2)	–
Orbit diameter	22.9 – 31.3 (27.6)	23.2 – 34.1 (27.8)	–
Upper jaw length	38.2 – 43.9 (41.9)	41.4 – 46.5 (44.2)	–
Head depth at midline orbit	47.2 – 58.3 (51.7)	50.4 – 59.9 (53.9)	–
Meristic data			
Dorsal fin rays (iii)	7	7	7#
Anal fin rays (iii)	11 – 12 (12)	11 – 12 (12)	11 – 12 (12)#

	Parazacco ignis (n=22)	*P. spilurus* (n=16)	*P. fasciatus* (n=13)
Pectoral fin rays (i)	13 – 14 (13)	13 – 14 (13)	–
Pelvic fin rays (i)	7 – 9 (7)	7 – 8 (7)	6*
Caudal fin rays (ii)	9+8	9+8	9+8#
Lateral line scales	40 – 45 (43)	45 – 50 (46)	41 – 44*
Scales above lateral line	8 – 9 (9)	9 – 10 (9)	–
Scales below lateral line	2 – 4 (3)	3 – 4 (3)	–
Pre-dorsal scales	19 – 22 (20)	21 – 24 (22)	–
Caudal peduncle scales	7 – 9 (8)	8 – 10 (9)	–
Tubercules on lower jaw	1 – 9 (2)	3 – 11 (4)	–
Vertebrae	20 – 22 + 19 – 21 = 41 (5), 42 (10), 43 (7)	19 – 21 + 20 – 21 = 41 (3), 42 (9), 43 (8)	20 – 22 + 19 – 21 = 39 (1), 40 (2), 41 (6), 42 (4)#

837 Table 3. Morphometric data for neotype and material of *Parazacco spilurus*. Numbers in
838 parentheses indicate the mean for morphometric data and mode for meristic data.

Measurement	Neotype	Material (n=19)
Total length (mm TL)	118.2	62.8 – 140.6 (101.7)
Standard length (mm SL)	99.2	50.9 – 122.9 (84.2)
Morphometric data		
% TL		
Head length	20.3	21.5 – 26.5 (23.2)
Body depth	22.6	17.3 – 22.4 (19.7)
% SL		
Head length	24.1	26.8 – 30.2 (28.1)
Body depth	26.9	21.0 – 26.4 (23.8)
Body width at dorsal origin	11.8	7.1 – 11.2 (8.7)
Body width at anal origin	10.0	5.7 – 8.3 (6.7)
Caudal peduncle depth	10.0	9.2 – 10.9 (9.8)
Caudal peduncle length	19.5	16.0 – 19.1 (18.0)
Pre-dorsal	53.6	51.1 – 54.3 (52.7)
Pre-anal	65.6	64.4 – 68.1 (66.5)
Dorsal origin to caudal base	47.9	43.5 – 49.1 (46.3)
Pectoral origin to pelvic insertion	25.9	24.2 – 27.5 (25.4)
Longest dorsal ray	18.9	17.1 – 21.4 (19.1)
Longest anal ray	26.3	17.8 – 34.9 (25.2)
Longest pectoral ray	19.8	15.6 – 22.3 (20.0)
Dorsal fin base	11.9	10.0 – 13.2 (11.3)
Anal fin base	15.9	12.1 – 16.3 (14.8)
Longest Pelvic fin ray	15.8	11.6 – 16.9 (15.4)
% HL		
Head width at nasal section	21.6	17.6 – 21.1 (19.9)
Snout length	33.8	28.7 – 36.0 (32.3)
Inter-orbital width	36.0	29.2 – 36.3 (31.9)
Orbit diameter	26.0	23.2 – 34.1 (27.9)
Upper jaw length	41.4	41.8 – 46.5 (44.3)
Head depth at midline orbit	59.9	50.4 – 56.3 (53.5)
Meristic data		
Dorsal fin rays (iii)	7	7
Anal fin rays (iii)	12	11 – 12 (12)
Pectoral fin rays (i)	13	13 – 14 (13)
Pelvic fin rays (i)	8	7 – 8 (7)
Caudal fin rays (ii)	9+8	9+8
Lateral line scales	45	45 – 50 (46)
Scales above lateral line	9	9 – 10 (9)
Scales below lateral line	3	3 – 4 (3)
Pre-dorsal scales	23	21 – 24 (22)
Caudal peduncle scales	8	8 – 10 (9)
Tubercules on lower jaw	9	3 – 11 (4)

Measurement	Neotype	Material (n=19)
Vertebrae	22 + 21 = 43	20– 22 + 20 – 22 = 41 (2), 42 (6), 43 (7)

884 Table 4. Morphometric data for holotype and paratypes of *Parazacco ignis*, new species.
885 Numbers in parentheses indicate the mean for morphometric data and mode for meristic data.

Measurement	Holotype	Paratypes (21)
Total length (mm TL)	118.7	64.3 – 110.5 (89.3)
Standard length (mm SL)	96.5	51.4 – 91.0 (72.7)
Morphometric data		
% TL		
Head length	23.2	22.1 – 24.6 (23.7)
Body depth	19.2	17.0 – 21.8 (19.1)
% SL		
Head length	28.5	27.6 – 30.9 (29.1)
Body depth	23.6	21.2 – 25.7 (23.5)
Body width at dorsal origin	10.6	7.2 – 11.4 (9.0)
Body width at anal origin	7.6	5.0 – 8.7 (6.8)
Caudal peduncle depth	10.2	9.3 – 10.8 (10.0)
Caudal peduncle length	17.4	15.1 – 18.8 (16.8)
Pre-dorsal	53.9	52.2 – 55.1 (53.5)
Pre-anal	67.6	65.1 – 70.6 (67.5)
Dorsal origin to caudal base	46.8	41.4 – 48.5 (45.0)
Pectoral origin to pelvic insertion	24.6	22.5 – 26.9 (24.6)
Longest dorsal ray	22.8	17.1 – 24.3 (20.5)
Longest anal ray	32.9	19.3 – 34.7 (24.4)
Longest pectoral ray	21.7	18.5 – 22.4 (20.6)
Dorsal fin base	12.6	10.0 – 13.1 (11.4)
Anal fin base	16.4	13.6 – 16.4 (14.8)
Longest Pelvic fin ray	17.5	13.9 – 18.3 (16.0)
% HL		
Head width at nasal section	19.7	17.0 – 22.3 (19.7)
Snout length	31.6	27.8 – 35.5 (31.8)
Inter-orbital width	33.6	29.0 – 33.8 (31.4)
Orbit diameter	24.7	22.9 – 31.3 (27.8)
Upper jaw length	41.6	38.2 – 43.9 (41.9)
Head depth at midline orbit	50.7	47.2 – 58.3 (51.8)
Meristic data		
Dorsal fin rays (iii)	7	7
Anal fin rays (iii)	12	11 – 12 (12)
Pectoral fin rays (i)	13	13 – 14 (13)
Pelvic fin rays (i)	7	7 – 9 (7)
Caudal fin rays (ii)	9+8	9+8
Lateral line scales	41	40 – 45 (43)
Scales above lateral line	8	8 – 9 (9)
Scales below lateral line	3	2 – 4 (3)
Pre-dorsal scales	21	19 – 22 (20)
Caudal peduncle scales	8	7 – 9 (8)
Tubercules on lower jaw	8	1 – 9 (2)
Vertebrae	22 +21 = 43	20 – 22 + 19 – 21 = 41 (5), 42 (10), 43 (6)

886